Xjenza Online - Science Journal of the Malta Chamber of Scientists
www.xjenza.org
DOI: 10.7423/XJENZA.2019.1.02

Research Article

A Preliminary Assessment of the Efficiency of Using Drones in Land Cover Mapping

Andrea Francesca Bellia[1] **and Sandro Lanfranco**[*1]
[1]*Department of Biology, University of Malta, Msida, Malta*

Abstract. This study represents a preliminary assessment of the efficiency of drones in surveying land cover at both large (*c.* 10 ha) and smaller (1 m^2) spatial scales. A DJI Mavic 2 drone was used to image the entire area of study and an orthomosaic was produced. This was converted into a land cover map through k-means clustering, with $k = 3$, where 'Vegetation', 'Bedrock' and 'Bare soil' corresponded to the land cover categories. Regions of interest (ROIs) were selected and subsequently surveyed from close range. The correspondence between predicted land cover (pLC) and observed land cover (oLC) was then assessed. On a large spatial scale, absolute correspondence was present between pLC and oLC. In terms of relative representation of land cover categories, 'Vegetation' was the only significantly correlated category across pLC and oLC, whilst the analogous correlations for 'Bedrock' and 'Bare soil' were weaker. The lower correspondence between pLC and oLC for 'Bedrock' and 'Bare soil' was due to the low value of $k = 3$ in the k-means clustering algorithm. This constrains a mixture of land covers into just one land cover category, with consequent reduction of the correlation between pLC and oLC. The method's accuracy and cost-effectiveness were compared to that of standard methods for land cover surveying. The entire process, including verification and orthomosaic land cover map processing times, approximated 32 hours. Consequently, this method is much shorter than standard surveys, which take days or weeks, and also requires less manpower.

Keywords: drone imagery, land cover mapping, vegetation mapping, image analysis, k-means clustering

1 Introduction

Amongst other uses, accurate land cover maps are a fundamental prerequisite for vegetation studies, ecological monitoring, geographical mapping, and land use planning. The spatial resolution of such maps depends on the purpose for which the map is intended, and on the size of the area under study. For coarse-grained mapping of large areas with relatively few land cover types, photographs taken from satellites or aircraft are usually useful (Anderson & Gaston, 2013; David & Ballado, 2016). Some satellites are also capable of much higher resolutions. The Sentinel-2 satellite is equipped with an opto-electronic multispectral sensor for surveying with a resolution of 10 to 60 m in the visible, near infrared (VNIR), and short-wave infrared (SWIR) spectral zones (https://eos.com/sentinel-2). However, if fine-grained mapping with a resolution of less than 10 m is required, aircraft and satellites would not be as useful, since their flight path would be too high and too fast, and their repeated use too costly (Anderson & Gaston, 2013). In summary, the data returned from these platforms would usually be too general to be relevant to the localised scales at which many ecological processes operate (Wulder, Hall, Coops & Franklin, 2004).

As such, the compilation of detailed land cover maps for smaller areas is often based on a bottom-up approach. For example, widely applied methods involve sampling using belt transects traversing the area (if an evident ecologically-relevant gradient is observed or suspected), in addition to using quadrat plots positioned at specific points. Such strategies enable direct characterisation of land cover within the sampling footprint, and interpolation of probable land cover in intervening areas that were not sampled directly. The design of a survey programme depends on the trade-off between the coverage required and the time and funds available. The use

**Correspondence to*: Sandro Lanfranco (sandro.lanfranco@um.edu.mt)

of more transects or quadrats would yield greater coverage, but at the expense of requiring more funds. Data collection is generally carried out on the ground by a team of expert field workers, with the effort required increasing with the size and ecological complexity of the area under study. As a result, the process is commonly time-consuming, effort-intensive and costly.

A possible solution to address the issues of cost, time, manpower and map detail, is the use of low altitude (< 500 m) aerial imagery to visualise an entire area of study, as well as specific regions of interest (ROIs) within it. The only affordable camera platform that can offer this versatility is a drone, a relatively small aircraft system that is remotely piloted through radio waves. Consumer-level drones with high quality photographic capability have recently increased in affordability and availability. This suggests that drones could represent a versatile and viable tool for mapping, since they can be used for surveying land-cover at the landscape scale, as well as at scales comparable to the dimensions of individual shrubs or trees.

2 Aims

This study represents a preliminary assessment of the efficiency of using a drone to survey land cover in an area of study, at both large (*c.* 10 ha) and smaller spatial scales (1 m^2). The large scale surveying will be used to generate an orthomosaic of the area of study, the accuracy of which would subsequently be validated against imagery captured from very low altitudes. The accuracy and cost-effectiveness of the method will be compared to that of standard methods for land cover surveying.

3 Materials and Method

3.1 Apparatus Used

All aerial imagery was captured using a DJI Mavic Pro 2 drone equipped with a Hasselblad L1D-20C camera, with 35 mm-equivalent focal length of 28 mm, a maximum lens aperture of f/2.8, and a Field of View (FOV) of approximately 77°. The CCD sensor was 13.2×8.8 mm in size and comprised of 20 million effective pixels. The size of the images produced was 5472×3648 pixels. The drone was flown using the proprietary RC unit connected to a Samsung Galaxy S9 smartphone, on which the Litchi app (flylitchi.com; VC Technology Ltd.) was running. This enabled live camera feed from the drone to be visible on the smartphone. A virtual grid with crosshairs intersecting at the centre of the camera's field of view was overlaid on the live camera feed in the Litchi environment, in order to facilitate positioning of the drone relative to specific targets.

3.2 The Area of Study

The study was carried out in an area of study (AoS) at Qasam Barrani, in the north-western part of Malta (Figs. 1 and 2). The primary and secondary axes of the AoS measured 330 m and 190 m respectively, covering an area of approximately 42 000 m^2. Land cover at the time of survey mainly consisted of a mosaic of perennial shrubs and grasses, tracts of exposed bedrock and patches of bare soil. A small number of anthropogenic constructions, including disused trapping hides and dry stone walls, were also present in the area.

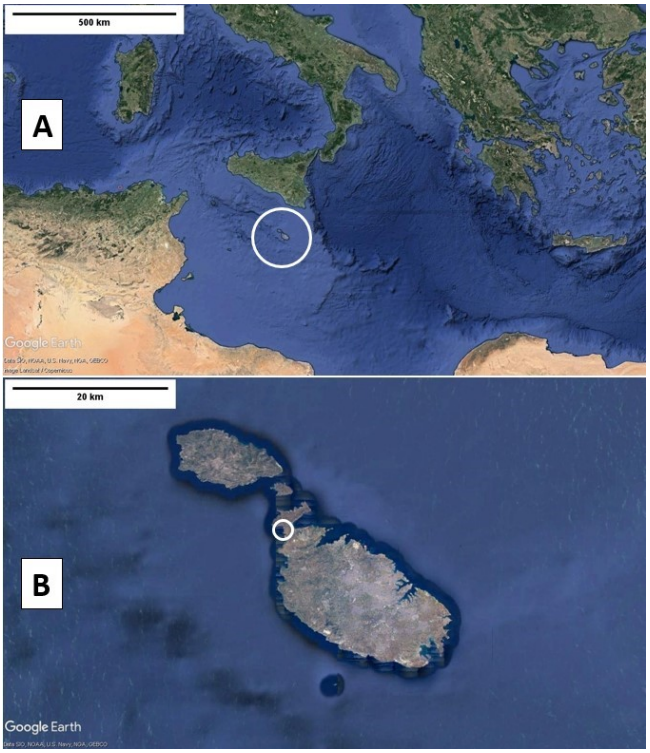

Figure 1: (A) General location, indicated by a white circle, of the Maltese Islands in the Central Mediterranean region. (B) Approximate location, indicated by a white circle, of the area of study in Malta. North is towards the top of the images. Base image: Google Earth.

3.3 Capture of Aerial Imagery

3.3.1 General Method

The mapping process was subdivided into three separate phases that were carried out sequentially. Phase 1 involved flying the drone at an elevation of approximately 30 m above ground in a number of parallel passes (henceforth referred to as 'transects') above the AoS, in order to capture the imagery required. These will subsequently be referred to as the 'high-altitude' images. Phase 2 was the processing stage, where the 'high-altitude' imagery was used to generate an orthomosaic. Phase 3 was the verification stage, where regions of in-

Figure 2: The AoS and its environs. The area that was surveyed is indicated by the red polygon. The blue rectangle indicates the boundaries of the actual area in which land cover was mapped. North is towards the top of the image. The red area covers *c.* 71 000 m^2 and the blue area covers *c.* 42 000 m^2.

terest (ROIs) noted in the orthomosaic were surveyed from a much lower altitude (5–10 m), in order to compare the predicted land cover with the observed land cover. The images captured during Phase 3 will subsequently be referred to as 'low-altitude' images. It should be emphasised that the land cover model produced is restricted to a local coordinate system, where only the distances between features within the model are considered. This model cannot be placed in an absolute geographic coordinate system as no ground control points (GCPs) were utilised. This decision was taken as there was no requirement to assess the area of study in the context of its surroundings, since the principal objective was to generate a map of the land cover in a localised area.

3.3.2 Calibration of FOV Area with Drone Altitude

Determination of the optimum survey altitude necessitated the calculation of the area covered by the camera's field of view (FOV) at different altitudes above ground level. The calibration process was carried out over a number of sessions in the grounds of the University of Malta.

The drone was flown above a car park in which the ground was marked with parking bays of known dimensions. The drone was piloted to the target altitude and photographs of the parking bays were taken in Digital Negative (DNG) RAW format. This format was selected in order to minimise any artefacts that may be introduced during compression to other formats such as JPEG. The target altitudes selected were 3 m, 5 m, 10 m, 15 m, 20 m, 25 m, 30 m, 35 m, 40 m, 45 m, 50 m, 75 m and 100 m above ground level.

Exchangeable image file format (EXIF) data was subsequently extracted from the metadata and used to record the relative altitude (calculated from the drone's barometric pressure sensor) at which each photograph was taken. The relative altitude sometimes deviated from the target altitude due to air turbulence experienced by the drone. The deviation between the relative altitude and target altitude was never larger than 0.1 m, equivalent to 0% to 0.67% of the target altitude. The images were subsequently processed in Image J v.1.52n (Schneider, Rasband & Eliceiri, 2012). The parking bay markings were used to calibrate the dimensions of each image, and the area covered by the FOV at each altitude was subsequently calculated using the area measurement tool of Image J. The calibration process was carried out independently on three occasions, with almost identical results (Fig. 3).

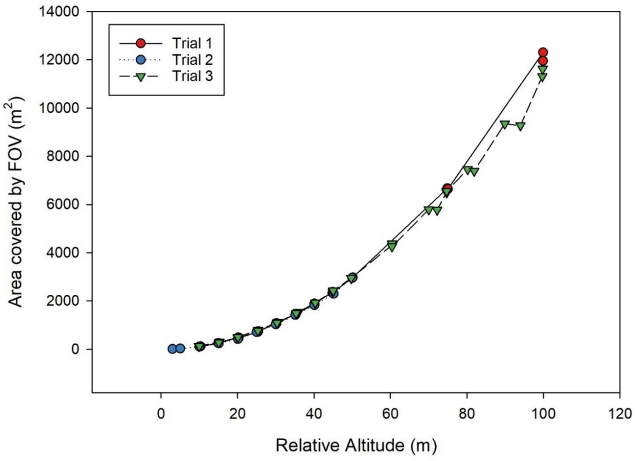

Figure 3: Calibration of the Field of View (FOV) of the drone with altitude above ground. The graph superimposes the results of three independent trials.

The Ground-Sampling Distance (GSD) of the drone camera, defined as the distance between pixel centres measured on the ground, was calculated for various altitudes using simple geometry. The GSD depends on the camera's focal length, on the width of the camera sensor, and on the altitude at which the drone is being flown. The variation in GSD, expressed in cm pixel^{-1}, with camera altitude is shown in Fig. 4.

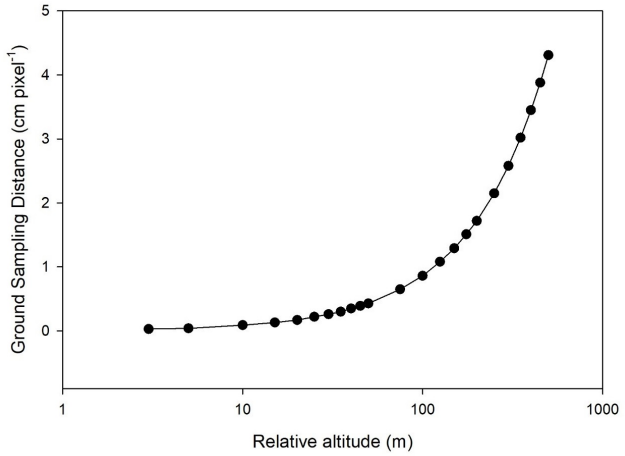

Figure 4: Variation in Ground Sampling Distance with altitude of drone camera above ground level.

3.3.3 Determination of Optimum Altitude for Survey

The optimum altitude for survey is dependent on the primary objectives of the survey. Identification of individual species would necessitate low-altitude surveys (3–10 m above ground level), whilst mapping of plant assemblages requires a larger FOV area and would therefore be carried out at higher altitudes (Putch, 2017). The altitude of survey also determines the minimum number of evenly-spaced transects that would be required to obtain sufficient overlap between transects, in order to allow orthomosaic maps to be compiled. After a number of trials, during which the drone was flown at different altitudes, a survey altitude of 30 m was noted to return images with sufficient detail for vegetation mapping, whilst remaining clear of all obstacles that were encountered, particularly trees. The spacing between transects was set to approximately 25–30 m, as this gave 49% overlap between images from neighbouring transects.

3.3.4 'High-Altitude' Image Capture

The flight paths along which the drone was flown during the survey were prepared on the online version of the Litchi app (flylitchi.com/hub). They were then uploaded to the drone at the time of survey. In the terminology used by Litchi, each survey flight constituted a 'Mission'. Missions were constructed using the 'Waypoints' tool in Litchi. These waypoints that the drone was set to visit were superimposed over a georeferenced base map showing the area of study (Fig. 5). The speed and height at which the drone would be flying were also predetermined and set for each waypoint. The drone was programmed to fly at an altitude of 30 m above the launching site at a constant speed of 5 km h^{-1}, taking photos in DNG format of the ground surface at 5 s intervals. Camera aperture and shutter speed were set automatically, depending on ambient conditions. This relatively slow speed of travel minimised the image blur sometimes observed when the drone travelled at higher speeds, or when the camera shutter was set to a relatively slow speed. The speed and height of flight were kept constant for each of the seven parallel transect belts that were required to cover the whole AoS.

The drone survey was carried out on 28 June 2019 between 0800 and 0845. The whole AoS was imaged over two sequential missions lasting 22 minutes and 15 minutes, respectively. The segmentation of the survey into two separate Missions was necessary as the drone's battery life was limited to approximately 30 minutes. This necessitated a change of battery between Missions. The area imaged by the drone was larger than the AoS in order to ensure that no parts of the AoS were omitted from the imaging process.

The distances between a number of distinctive ground markers, including large rocks and anthropogenic structures, were measured in the field in order to enable calibration of the drone image during the processing phase.

3.4 Processing of Aerial Imagery

The 378 'high-altitude' images obtained from the drone were initially processed in Affinity Photo v.1.7 to remove lens distortion (Kim, Lee & Choi, 2015), and were subsequently imported into Agisoft Metashape Professional version 1.5.4 in order to generate an orthomosaic of the whole AoS. The process involved alignment of the photos, setting of a scale based on the relative positions of fixed ground markers, building of the dense cloud of points, building of the mesh, rendering of the texture, and exportation of the orthomosaic. The workflow is summarised in Fig. 6. The entire processing step required approximately 24 hours on the computer hardware available (Dell G5 5587, hexacore Intel Core i7-8750H processor, 16 GB RAM).

3.5 Segmentation of Orthomosaic

The orthomosaic was processed in order to generate a pseudocolour land cover map. Preliminary surveys of the orthomosaic had suggested that an initial segmentation of the image into three land cover categories would have been reasonable. The three categories selected were 'Vegetation', 'Bedrock' and 'Bare Soil'. In this preliminary study, the 'Vegetation' land cover category was not subdivided into different species or lifeforms, as this would have required multi-seasonal studies over several years. However, the initial results suggest that this would be feasible. The image was subsequently segmented using the k-means clustering plugin in Image J, with the value of $k = 3$, since three land cover categories were defined. This algorithm assigned each pixel in

Figure 5: Path of drone transects over the area of study, as constructed in the Litchi app. The survey was split into two missions since a battery change was required after 25 minutes.

the image to an intensity value of 0, 1, or 2, depending on the intensity of its neighbouring pixels. This created an image with three distinct regions, each region presumably corresponding to one of the three land cover categories. For better visibility and to facilitate interpretation, this image was converted into a pseudocolour image by editing its lookup table and changing each of the three coverages into a primary colour (blue, green and red).

3.6 Verification

The effectiveness of the pseudocolour land cover map in predicting actual land cover categories in the field was then assessed. Inspection of the land cover map indicated 14 ROIs of varying areas in which there was either a preponderance of one of the three land cover categories, or in which an approximately symmetrical mixture of land cover was present. These ROIs were selected as areas in which the correspondence between the predicted land cover and observed land cover would be assessed. Each ROI was cropped out of from the land cover map. The relative proportion of 'Bedrock', 'Bare Soil' and 'Vegetation' cover in each ROI was determined by saving the cropped section as a text image. The number of pixels in each of the three land cover categories were enumerated and expressed as a proportion of the number of pixels in the cropped image. The land cover values obtained for each ROI are henceforth referred to as the 'predicted land cover' (pLC).

In order to measure the observed land cover, a Mission was created in which the drone was programmed to fly to each ROI, hover at an altitude ranging from 5–10 m above its central point, depending on the terrain, and record a 'low-altitude' ground photo. The altitude of the drone allowed the area of the FOV to be read off from the graph in Fig. 3. Therefore, on 2 July 2019 each of the 14 ROIs were visited and the programmed Mission implemented. The photo resolution of each ROI was such that dominant plant species identification was straightforward. The relative proportion of 'Bedrock', 'Bare Soil' and 'Vegetation' cover in each ROI photo was determined through image segmentation using k means clustering ($k = 3$) and verified through visual inspection. These values are referred to as the 'observed land cover' (oLC).

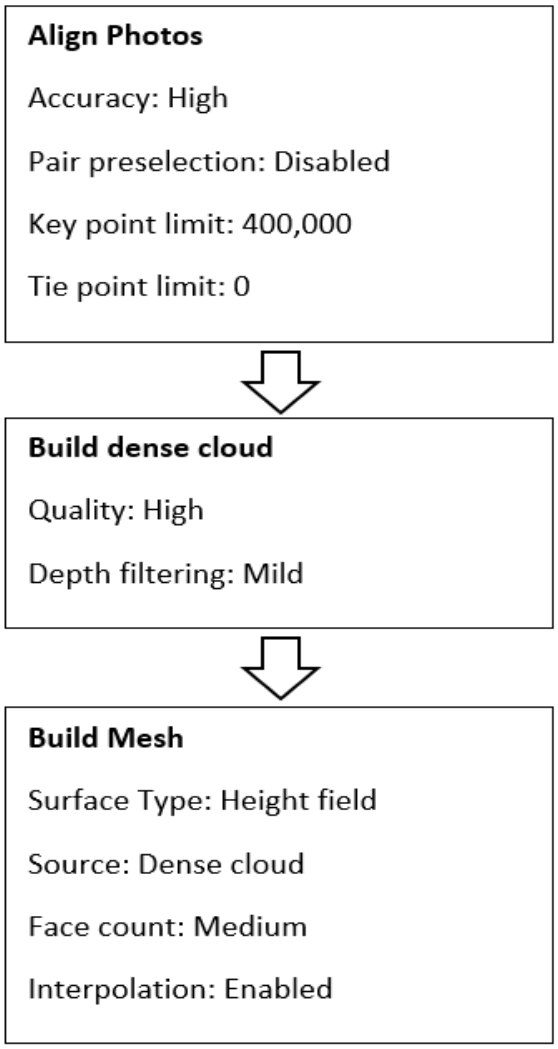

Figure 6: Summary of workflow followed during image processing phase.

3.7 Analysis of Data

The correspondence between the pLC and oLC values was tested by calculating the Pearson Product Moment Correlation Coefficient, after ensuring that the data was parametric. The relative contribution of the three land cover categories to differences within and between the pLC and oLC vales was assessed through Principal Component Analysis in Canoco v.5.12 (ter Braak & Šmilauer, 2018).

4 Results

4.1 Orthomosaic Map

The colour orthomosaic map of the AoS and its environs that was stitched from the 378 drone photos is shown in Fig. 7.

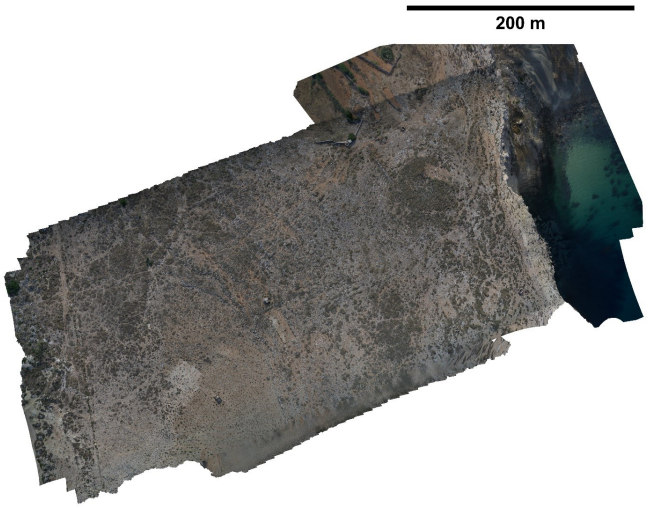

Figure 7: Orthomosaic map of the area of study and its environs. This image was stitched from 378 photos. The scale is given at the top right.

4.2 Land Cover Map

The Red-Green-Blue pseudocolour land cover map of the AoS is shown in Fig. 8. Every pixel in the orthomosaic was constrained to one of three intensity values that were subsequently converted into primary colours. The blue pixels represent 'Vegetation', red pixels are 'Bare soil' and green pixels are 'Bedrock'. The approximate positions of the 14 ROIs used for verification are indicated.

4.3 Correlation Between pLC and oLC

4.3.1 Presence-Absence of Land Cover Categories

When considering the binary presence or absence of land cover categories in each ROI, the overlap between the paired pLC and oLC in each ROI was complete. The oLC of every ROI matched the corresponding pLC.

4.3.2 Relative Coverage of Land Cover Categories

When the relative coverage of each land cover category in the ROIs was taken into account (Table 1), the correlations between the paired pLC and oLC were less pronounced (Fig. 9). Pearson product-moment correlation coefficients for the land cover categories were not statistically significant for any of the land cover categories (Table 2). When potential outlier ROI-7 was removed from the analysis, the correlation between the pLC and oLC for 'Vegetation' was statistically significant ($r = 0.568$, $p = 0.04$, $n = 13$). The corresponding correlations for 'Bedrock' and 'Bare soil' remained below the threshold of statistical significance.

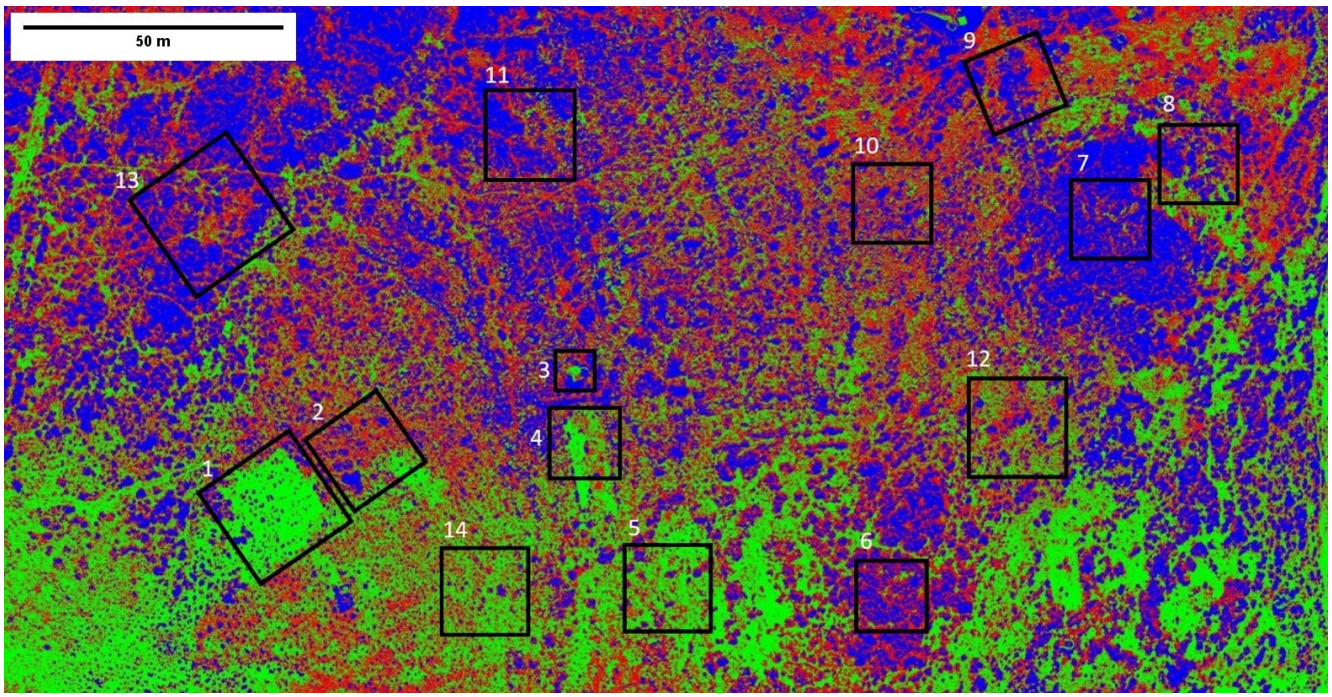

Figure 8: Pseudocolour map of the area of study segmented into three regions: 'Vegetation' (blue), 'Bare soil' (red) and 'Bedrock' (green).

Table 1: Predicted and observed land cover in the 14 ROIs.

ROI	Vegetation (predicted)	Vegetation (observed)	Bare soil (predicted)	Bare soil (observed)	Bedrock (predicted)	Bedrock (observed)
ROI_01	0.157	0.230	0.248	0.420	0.595	0.350
ROI_02	0.127	0.340	0.386	0.390	0.488	0.280
ROI_03	0.344	0.300	0.365	0.340	0.291	0.360
ROI_04	0.163	0.250	0.358	0.580	0.478	0.170
ROI_05	0.093	0.290	0.285	0.350	0.622	0.360
ROI_06	0.414	0.430	0.458	0.230	0.128	0.340
ROI_07	0.729	0.350	0.250	0.260	0.021	0.400
ROI_08	0.384	0.430	0.355	0.300	0.261	0.270
ROI_09	0.486	0.320	0.451	0.400	0.063	0.280
ROI_10	0.424	0.300	0.500	0.280	0.076	0.420
ROI_11	0.504	0.430	0.419	0.260	0.077	0.310
ROI_12	0.239	0.370	0.434	0.320	0.327	0.310
ROI_13	0.504	0.450	0.436	0.270	0.060	0.280
ROI_14	0.089	0.360	0.385	0.370	0.527	0.270

The data were further analysed using Principal Component Analysis (PCA), with potential outlier ROI-7 omitted (Fig. 10). The relative arrangement of ROIs on the PCA plot suggested that there was no particular correspondence in relative land cover composition between the paired pLC and oLC from each ROI. Moreover, the variation in relative land cover composition was much higher for the pLC than it was for the oLC. The maximum axis of variation of the convex hull, representing the pLC ROIs, coincided with the maximum axis of variation of the PCA plot (Axis I). Axis I of the PCA plot was most strongly correlated with the 'Bedrock' land cover category, suggesting considerable variability in assessment of this land cover category from the main orthophoto mosaic. Conversely, the oLC ROIs were mainly dispersed parallel to Axis II, which accounted for a much lower proportion of the total variation in the dataset. The 'Bare soil' and 'Vegetation' vectors were strongly correlated with Axis II.

Table 2: Pearson correlation (r) between predicted and observed land cover in each category. Data derived from the 14 ROIs. The statistical significance (p) and sample size (n) are given.

LC Category	r	p	n
Vegetation	0.467	0.090	14
Rock	−0.276	0.339	14
Soil	−0.270	0.350	14

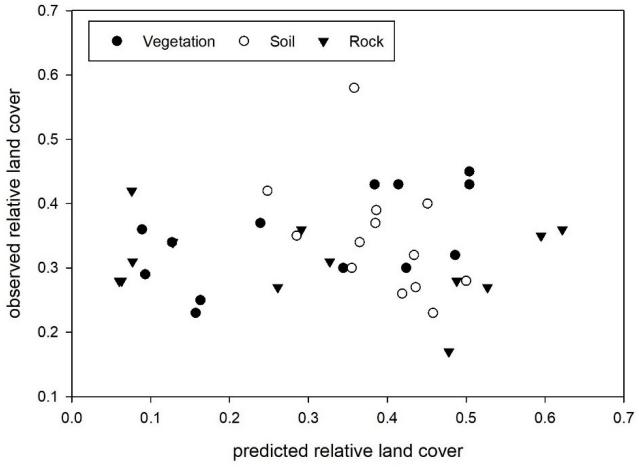

Figure 9: Correlation between the predicted and observed cover of the three land cover categories in each of the 14 ROIs. The ROI labels have not been included as these would have diminished the readability of the figure.

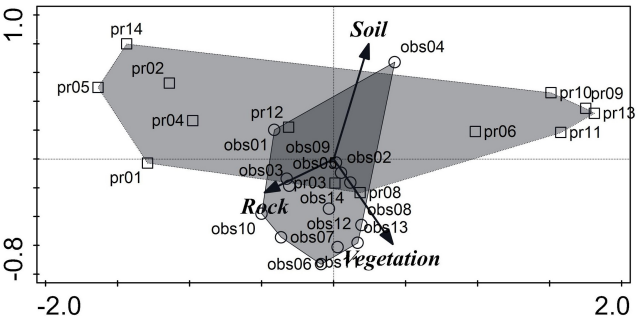

Figure 10: PCA ordination plot of the predicted and observed land cover in the 14 ROIs. Axis I and Axis II account for 83.62% and 12.59% of the variability of the data respectively.

5 Discussion

5.1 Correspondence Between Predicted and Observed Land Cover

Correspondence between the pLC and oLC was absolute when considered on a presence-absence basis. Although this may initially be perceived as a positive result, it should be emphasised that the land cover in the AoS was distributed in a mosaic pattern, and that this correspondence was not significantly different from a random pattern.

In terms of relative representation of the three land cover categories in each ROI, the only category that was significantly correlated across pLC and oLC was 'Vegetation'. This is a consequence of the optical reflectivity properties of plant foliage, which, in the AoS, reflected less light than other types of land cover and was therefore very distinct. Conversely, the optical distinction between 'Bedrock' and 'Bare soil' was much weaker as the soil in the AoS is similar to the parent rock. Furthermore, much of the soil is armoured with cobbles that are derived from the bedrock and therefore, in terms of reflectivity, are indistinguishable from it. Some regions of the land cover map that were interpreted as being covered by 'Bare soil' were actually characterised by 'Bedrock' mantled with a very shallow layer of gravel.

This raises a question regarding the choice of land cover categories. The sharp distinction between land cover categories that was evident in the land cover map was not observed in the field, where there was no clear boundary between 'Bedrock' and 'Bare soil'. The distinction in the land cover map was a consequence of the value of k in the clustering algorithm, as each pixel was constrained into one of only three discrete values. This therefore created abrupt boundaries that muted the range of intermediate land covers which were actually observed in nature.

This may also account for the much higher variability in the pLC data, relative to the oLC data. ROIs that may have been characterised by a high diversity of land cover categories at a large scale, turned out to be much less varied when examined at closer range. Once again, this is attributable to the optical distinction between 'Bedrock' and 'Bare soil'. In many cases, ROIs that were predicted to have relatively high 'Bare soil' cover were in fact observed to be characterised by relatively high 'Bedrock' cover, when examined from close range at low altitudes.

The 'Vegetation' category was less equivocal, although different species could obviously not be distinguished from each other when the value of k was too low for that to be feasible.

The optical characteristics of the 'Vegetation' category are also likely to vary considerably with season. The onset of the wet season would be correlated with the development of new foliage in perennial plants and the emergence of annual plants. This implies that much of the area categorised as 'Bare soil' would transition to 'Vegetation' during the wet season, reducing the land cover diversity of individual ROIs. In this situation, a value of $k = 3$ might no longer represent the optimum number of land cover categories. As such, this suggests that in order to give a more complete assessment of the efficiency of drone-based surveys, the study should be

repeated in different seasons, and preferably over several years.

5.2 Efficiency of the Method

5.2.1 Duration

The duration of the entire process, including verification and processing time for production of the orthomosaic and land cover map, was approximately 32 hours. This duration is much shorter than that required for a standard survey that produces the same output, where the comparable figure is several days or weeks.

5.2.2 Manpower and Expertise

The manpower requirements were also significantly lower, since the whole study was carried out by two persons (the authors), and could certainly be carried out by one. The comparable manpower requirements for a standard survey and map production would usually be higher, with one or two persons carrying out the field survey and at least one person producing the land cover maps. The level of expertise required to pilot a drone is probably not a major limiting factor. Although both authors had each flown well over a hundred Missions prior to conducting the present study, the level of expertise required to implement the Missions for the present study did not require that level of experience.

5.2.3 Cost

If the initial capital costs for the drone and computer hardware and software are excluded, the method tested during this study is more cost effective, less labour intensive and much more rapid than standard methods of field survey. It also generated a land cover map with a spatial resolution that would have required several weeks or months for a standard survey team to produce. However, it should be stressed that the present study did not attempt to place the land cover model in an absolute coordinate system and was only based on relative local coordinates. Locating the land cover model in an absolute frame of reference would have increased the cost considerably, as this would have necessitated the use of ground control points (GCPs) and determination of their precise geographic position. This process would require input from more personnel and would also necessitate the use of very costly equipment. Although the surveying equipment would represent a (considerable) one-time cost, the use of trained personnel to set the GCPs and determine their position would be recurring. As such, the cost-effectiveness of the method should be seen in this light.

5.3 Conclusions

The proposed method, as tested during the present study, highlighted several limitations of using a drone to survey land cover. However, almost all of these limitations were attributable to choices made at the processing stage. The drone imagery was detailed enough to permit identification of individual plant species from a low altitude, and of distinct assemblages from higher altitudes.

The relatively low correspondence between pLC and oLC, particularly for 'Bedrock' and 'Bare soil', was a consequence of the low value of $k = 3$ in the k-means clustering algorithm. This implies that patches of land comprising a mixture of land covers would be constrained into just one land cover category, with consequent reduction of the correlation between pLC and oLC. The low resolution returned by the clustering algorithm was a choice made by the authors and does not represent an inherent shortcoming of the proposed method. A higher value of k would have increased the resolution of the land cover map, but would have increased the probability of generating spurious land cover categories.

All in all, the utility of the land cover map depends on the purpose for which it was created. A survey of plant communities would be likely to require $k > 3$ to permit the identification of different assemblages, whilst for a binary survey of agricultural land use, $k = 3$ would probably suffice.

The preliminary study presented here suggests that $k = 3$ gives good correspondence at a large spatial scale, but is less accurate at smaller spatial scales. Nevertheless, for many purposes, it is the larger spatial scales that are of interest, and the performance of the land cover map at this larger scale was certainly satisfactory, compared to maps produced by standard survey methods. If information at smaller spatial scales is required, then using $k > 3$ will be necessary to highlight transitional land covers that may not be relevant at larger scales.

Acknowledgements

We would like to thank Amber Dimech, Emily Farrugia and Julia Scerri, interns at the Department of Biology, University of Malta, for field assistance.

References

Anderson, K. & Gaston, K. J. (2013). Lightweight unmanned aerial vehicles will revolutionize spatial ecology. *Front. Ecol. Environ. 11*(3), 138–146.

David, L. C. G. & Ballado, A. H. (2016). Vegetation indices and textures in object-based weed detection from UAV imagery. In *Proceedings of the 2016 6th IEEE International Conference on Control System, Computing and Engineering (ICCSCE)* (pp. 669–674). Batu Ferringhi, Malaysia: IEEE.

Kim, B.-J., Lee, Y.-K. & Choi, J.-K. (2015). Investigating applicability of unmanned aerial vehicle to the

tidal flat zone. *Korean J. Remote Sens. 31*(5), 461–471.

Putch, A. (2017). *Linear Measurement Accuracy of DJI Drone Platforms and Photogrammetry.* San Francesco: DroneDeploy.

Schneider, C. A., Rasband, W. S. & Eliceiri, K. W. (2012). NIH Image to ImageJ: 25 years of image analysis. *Nat. Methods*, *9*(7), 671–675.

ter Braak, C. J. F. & Šmilauer, P. (2018). *Canoco reference manual and user's guide: software for ordination (version 5.10).* Wageningen: Biometris, Wageningen University & Research.

Wulder, M. A., Hall, R. J., Coops, N. C. & Franklin, S. E. (2004). High Spatial Resolution Remotely Sensed Data for Ecosystem Characterization. *Bioscience*, *54*(6), 511–521.